Supplementary Figures and Table

Myelin-specific CD8 T cells exacerbate brain inflammation in CNS autoimmunity

Catriona A. Wagner[1], Pamela J. Roqué[1], Trevor R. Mileur[1], Denny Liggitt[2], and Joan M. Goverman[1*]

[1]Departments of Immunology and [2]Comparative Medicine, University of Washington, Seattle, WA, USA

Correspondence should be addressed to Joan M. Goverman (goverman@uw.edu)

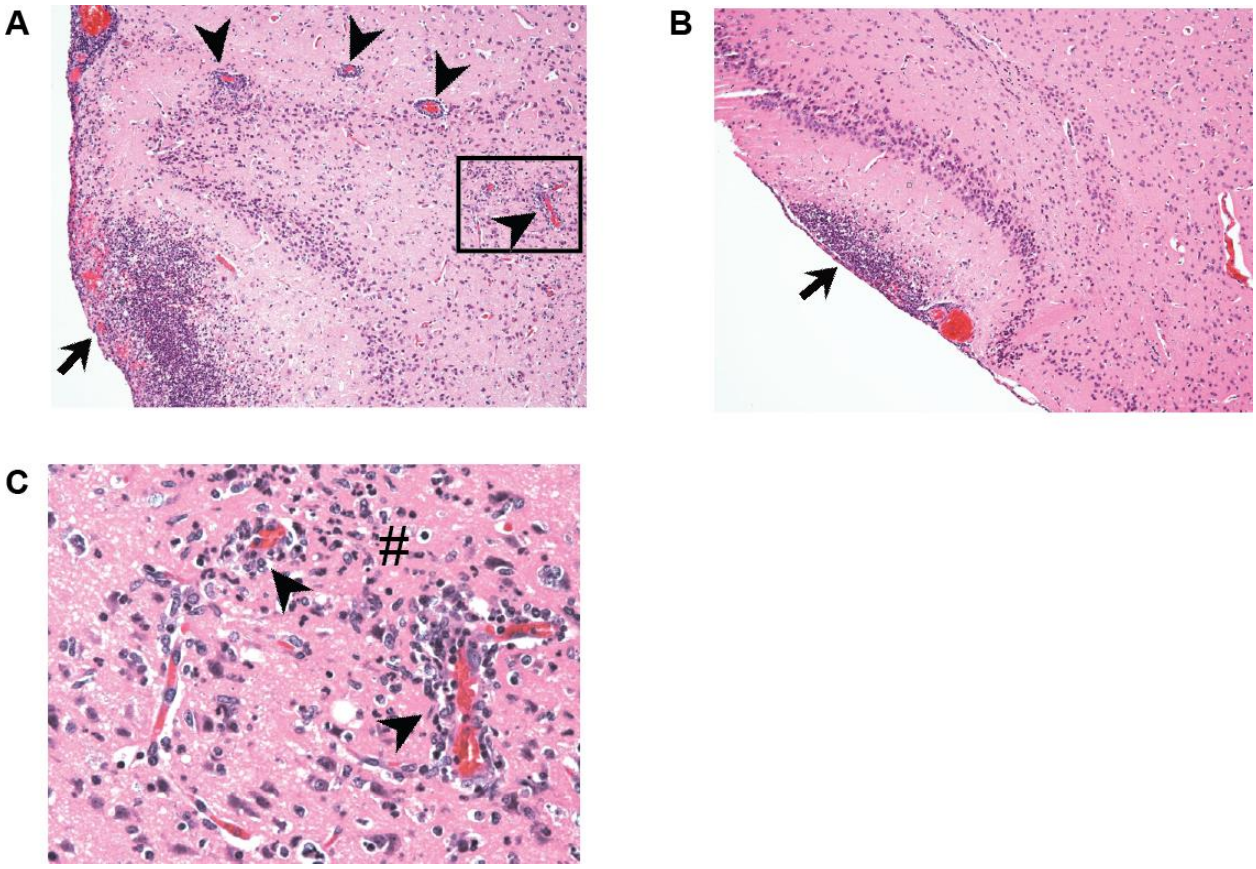

Supplementary Figure 1. MBP-specific CD8 T cells enhance the lesion severity and increase the frequency of parenchymal vessel-associated lesions in the brain during CD4-initiated EAE. Histopathology is shown for representative brain sections from the cortical region caudal to the olfactory bulb harvested from mice 7 days post-CD4 T cell transfer that had received (**A** and **C**) 8.8 or (**B**) WT CD8 T cells. (**A** and **B**) Lesions in both groups demonstrate substantial necrotizing lesions involving the meninges and submeningeal regions (arrows). However, lesions in CD4-initiated/$CD8_{8.8}$ EAE mice (**A**) have additional complexity in that perivascular and closely associated parenchymal areas distal from the site of meningeal involvement (arrowheads) are more frequently observed, and have focal accumulations of neutrophilic and mononuclear inflammatory cells. (**C**) Higher power magnification of the boxed area in (**A**) shows perivascular inflammatory cell cuffing (arrowheads) along with parenchymal inflammatory cell accumulations (hash mark). Original magnification for (**A** and **B**) is 10x and (**C**) is 40x. Data are representative of 12 mice per group from 2 independent experiments.

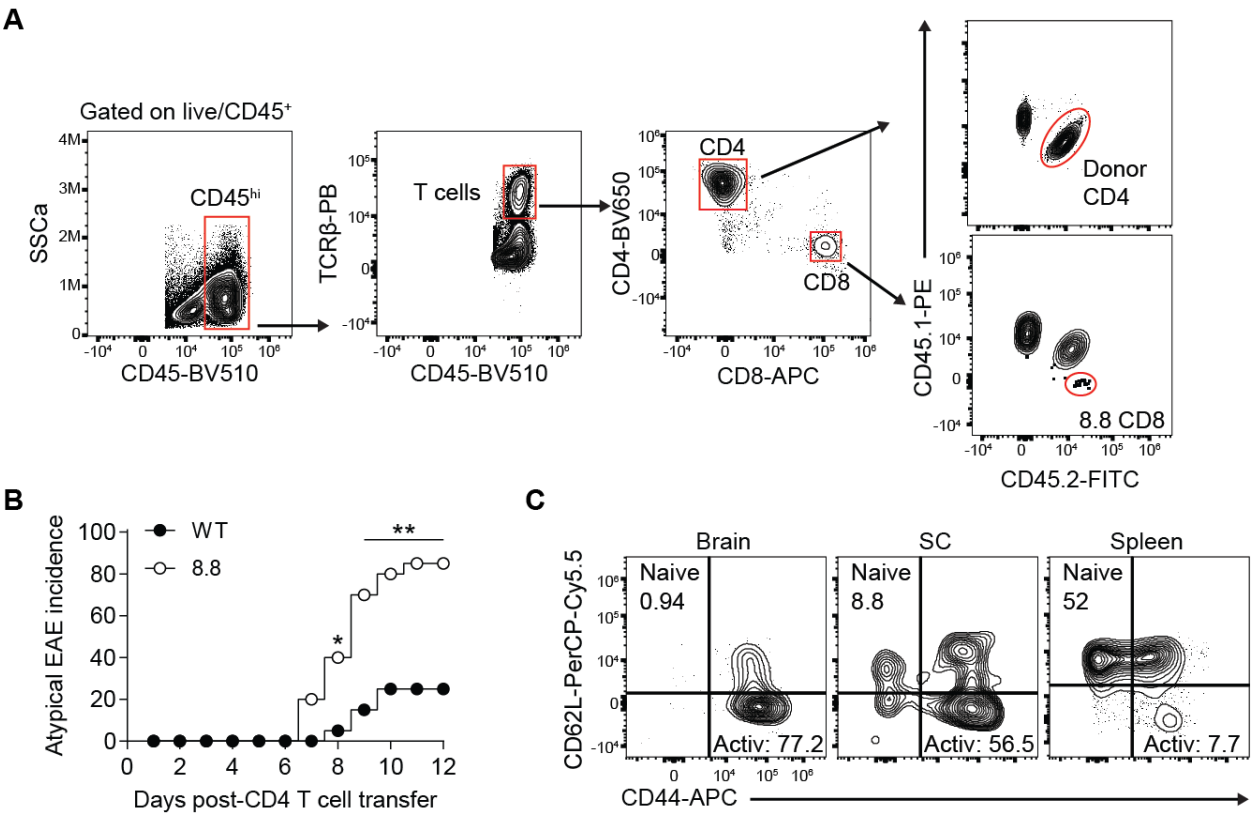

Supplementary Figure 2. 8.8 CD8 T cell accumulate and acquire an activated phenotype in the brain during CD4-initiated EAE. (**A**) EAE was induced by transferring CD45.1.2^{+} MOG-specific CD4 T cells into CD45.1.1^{+} mice that had received CD45.2.2^{+} 8.8 CD8 T cells. Gating strategy used to identify CD45^{hi} cells, donor CD4 T cells and 8.8 CD8 T cells is shown for mononuclear cells isolated 7 days post-CD4 T cell transfer from the brain of a mouse with atypical EAE. Cells are initially gated on single, live, CD45^{+} cells. (**B**) EAE was induced by transferring MOG-specific CD4 T cells into either WT or intact 8.8 mice. The percentage of mice exhibiting atypical EAE signs at the indicated days post-CD4 T cell transfer is shown (n=20 per group; 3 independent experiments). (**C**) EAE was induced by transfer of CD45.1.1^{+} MOG-specific CD4 T cells into CD45.2.2^{+} intact 8.8 mice. Mononuclear cells were isolated from the brain, spinal cord and spleen 7 days post-CD4 T cell transfer and expression of CD44 and CD62L was analyzed by flow cytometry. Representative flow cytometry of activated (CD44^{hi}CD62L^{lo}) or naïve (CD44^{lo}CD62L^{hi}) 8.8 CD8 T cells. Data are representative of 2 independent experiments (n=12). (**B**) Statistical significance was determined using a Fisher's Exact test. * $p<0.05$, ** $p<0.01$.

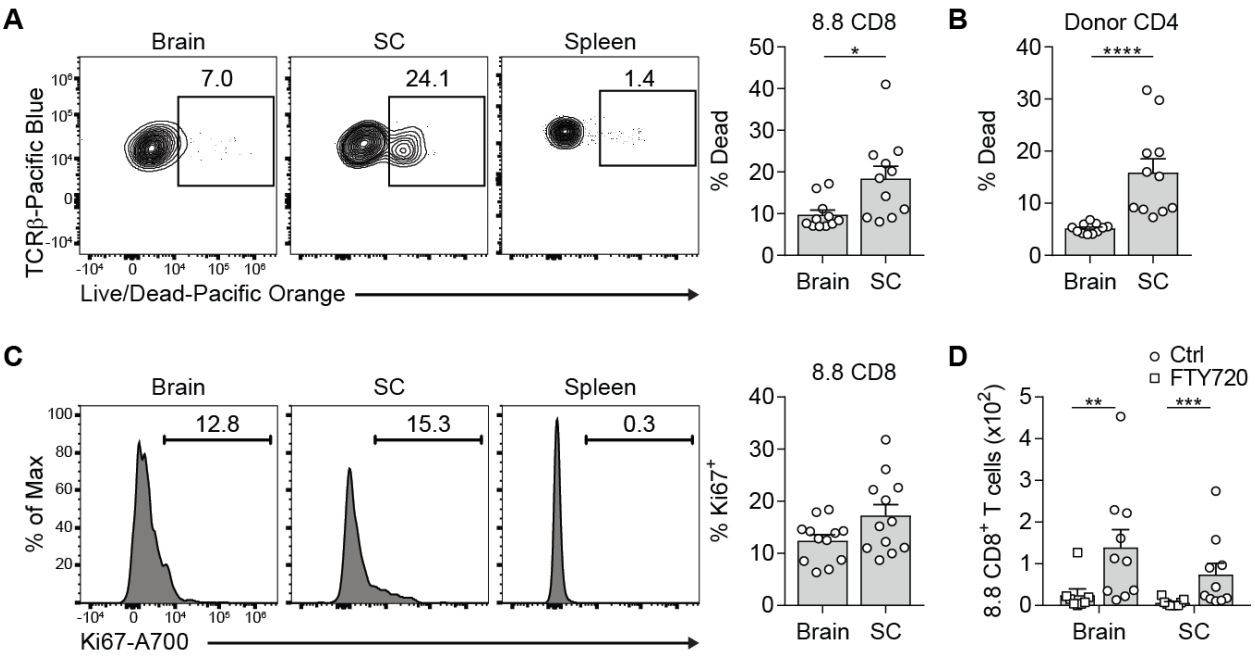

Supplementary Figure 3. 8.8 CD8 T cell accumulation in the brain does not reflect differences in their recruitment, proliferation or cell death in different regions of the CNS. (**A-C**) EAE was induced by transfer of CD45.1.1$^+$ MOG-specific CD4 T cells into CD45.2.2$^+$ intact 8.8 mice. Mononuclear cells were isolated from the brain, spinal cord and spleen 7 days post-CD4 T cell transfer and cell death and proliferation were analyzed by flow cytometry using a cell-impermeable amine-reactive dye (Succinimidyl Ester) and Ki67, respectively. (**A**) Representative flow cytometry and frequency of dead 8.8 CD8 T cells and (**B**) frequency of dead donor CD4 T cells in the indicated tissues is shown. (**C**) Representative flow cytometry and frequency of Ki67$^+$ 8.8 CD8 T cells in the indicated tissues is shown. (**D**) EAE was induced by transferring CD45.1.2$^+$ MOG-specific CD4 T cells into CD45.1.1$^+$ mice that received CD45.2.2$^+$ 8.8 CD8 T cells one day earlier. FTY720 or vehicle control were injected 6 days post-CD4 T cell transfer into mice that had received 8.8 CD8 T cells. The numbers of 8.8 CD8 T cells in the brain and spinal cord were determined on day 7 by flow cytometry. Graphs show mean + SEM (one symbol per mouse) and are compiled from two independent experiments with at least n=8 mice per group. Statistical significance was determined using a Mann-Whitney *U* test. * p<0.05, ** p<0.01, *** p<0.001, **** p< 0.0001.

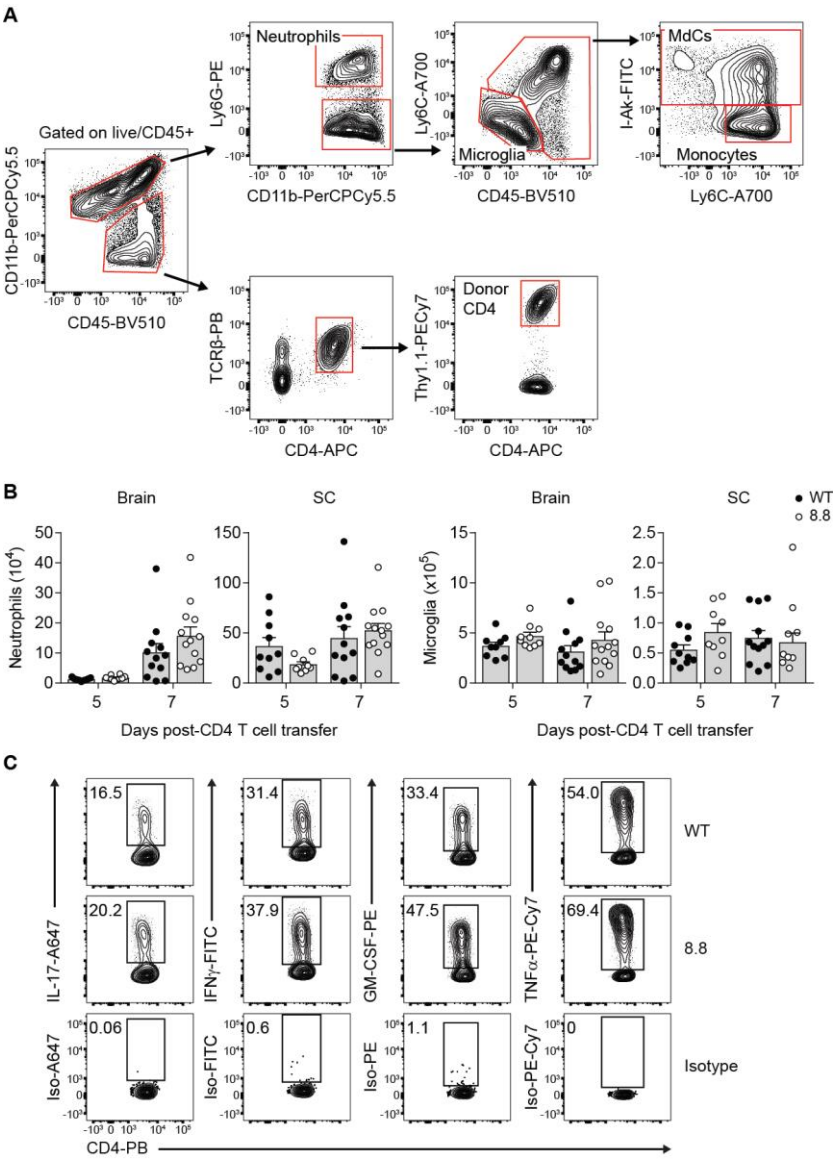

Supplementary Figure 4. Gating strategy to identify different immune cell subsets in the CNS and cytokine production by donor CD4 T cells. EAE was induced by transferring Thy1.1$^+$ MOG-specific CD4 T cells into Thy1.2$^+$ mice that received Thy1.2$^+$ WT or 8.8 CD8 T cells one day earlier. (**A**) Representative flow cytometry is shown for mononuclear cells isolated 7 days post-CD4 T cell transfer from the brain of a mouse with atypical EAE. Gates used to identify different immune cell subsets are shown. Cells are initially gated on single, live, CD45$^+$ cells. (**B**) The numbers of neutrophils and microglia were determined by flow cytometric analyses on days 5 (WT: n=9; 8.8: n=10) and 7 (WT: n=12; 8.8: n=13) post-CD4 T cell transfer. (**C**) Mononuclear cells were isolated 7 days post-CD4 T cell transfer and were stimulated with MOG_{97-114} peptide prior to intracellular cytokine staining. Representative flow cytometry of cytokine-producing donor CD4 T cells isolated from the brain of a mouse that received 8.8 CD8 T cells is shown. Data are representative of 2 independent experiments (WT: n=10; 8.8: n=9). Graphs show mean + SEM (one mouse/symbol) and are compiled from at least 2 independent experiments. Statistical significance was determined using a Mann-Whitney *U* test.

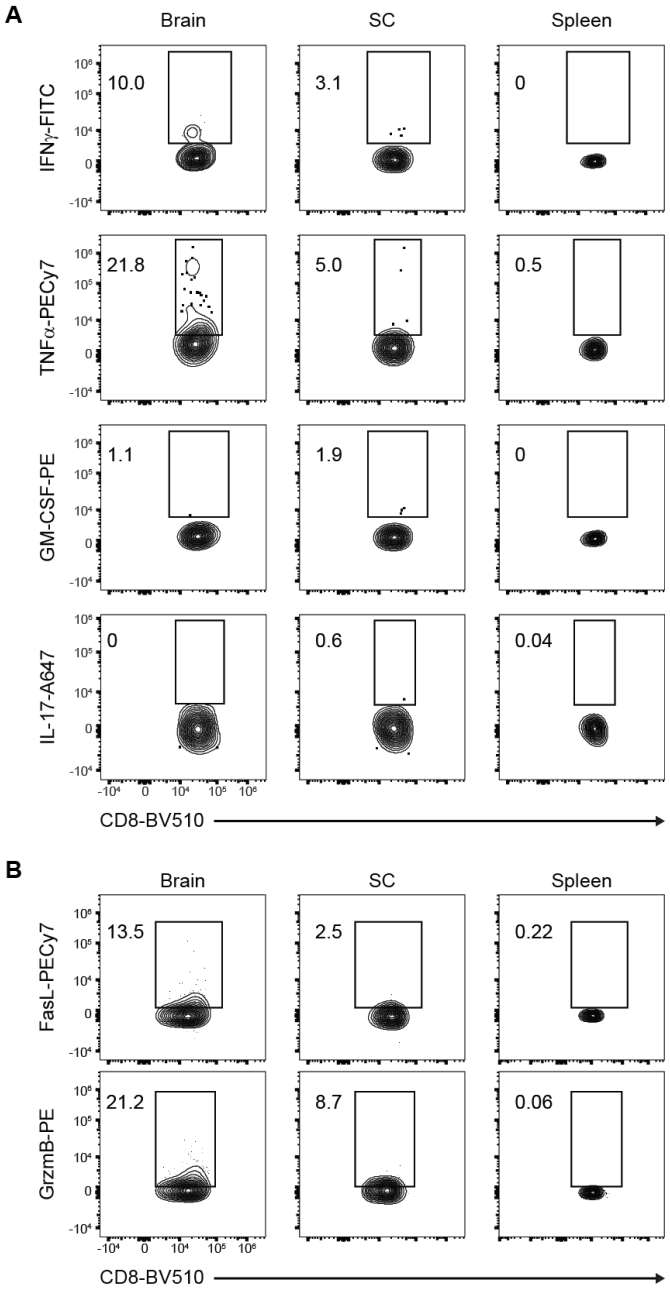

Supplementary Figure 5. Phenotypic analyses of CNS-infiltrating 8.8 CD8 T cells. EAE was induced by the transfer of CD45.1.1^{+} MOG-specific CD4 T cells into CD45.2.2^{+} intact 8.8 mice. Mononuclear cells from the brain, spinal cord (SC), and spleen were analyzed by flow cytometry on day 7. All analyses are gated on 8.8 CD8 T cells (CD45^{+}TCRβ^{+}CD8^{+}CD45.2.2^{+}). (**A**) Mononuclear cells were incubated with GolgiPlug without stimulation prior to intracellular cytokine staining for cytokines. Representative flow cytometry showing IFNγ, TNFα, GM-CSF and IL-17 expression by 8.8 CD8 T cells (n=10). (**B**) Representative flow cytometry showing FasL and granzyme-B (GrzmB) expression by 8.8 CD8 T cells (n=12). All data are representative of 2 independent experiments.

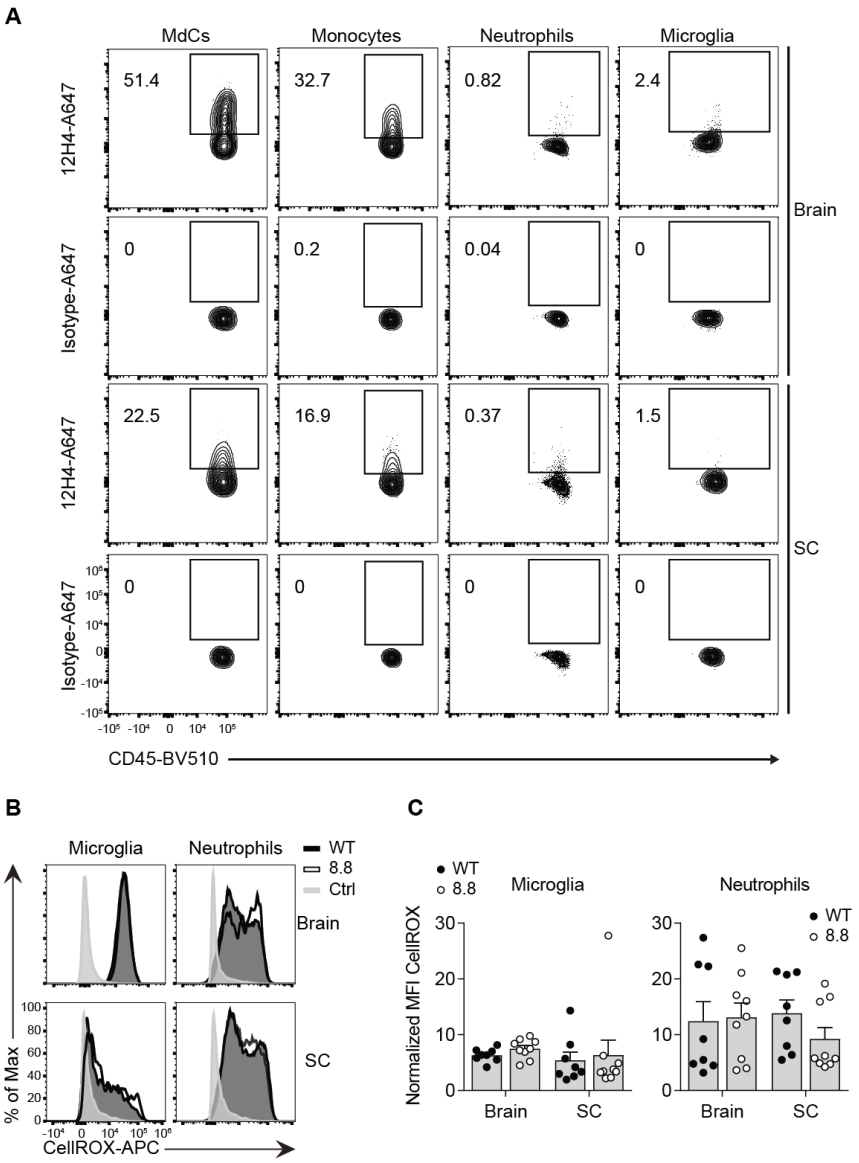

Supplementary Figure 6. MdCs and monocytes, and not neutrophils or microglia, are the predominant cell-types presenting MBP/K^k in the brain and spinal cord. (**A**) EAE was induced by transferring MOG-specific CD4 T cells into WT mice. Mononuclear cells were isolated from the brains and spinal cords (SC) of mice on day 7 post-CD4 transfer. Representative flow cytometry plots of MBP/K^k-specific 12H4 antibody and isotype control staining gated on MdCs, monocytes, neutrophils, and microglia are shown. Data are representative of 2 independent experiments (n=10). (**B** and **C**) EAE was induced by transferring MOG-specific CD4 T cells into WT mice that had received either WT or 8.8 CD8 T cells one day earlier. Mononuclear cells were isolated from the brains and spinal cords (SC) and analyzed by flow cytometry. (**B**) Representative flow cytometry and (**C**) MFIs (medians) of microglia and neutrophils CellROX staining are shown for CNS tissues harvested on day 7 post-CD4 T cell transfer. Data are representative of 2 independent experiments (WT: n=8, 8.8: n=9). Expression of CellROX by T cells was used as a negative control (Ctrl) to generate normalized MFI values. (**C**) Graphs show mean + SEM (one symbol per mouse). Statistical significance was determined using a Mann-Whitney *U* test.

Supplementary Table 1. Primers used for qRT-PCR.

Gene	Forward primer (5'-3')	Reverse primer (5'-3')
Ccl2	TGG GCC TGC TGT TCA CAG TT	TGG GGC GTT AAC TGC ATC TGG
Ccl3	ACC AAG TCT TCT CAG CGC CA	GTC AGG AAA ATG ACA CCT GGC TG
Ccl4	AGC CAG CTG TGG TAT TCC TGA C	TCT CCT GAA GTG GCT CCT CCT
Ccl5	TCA CCA TAT GGC TCG GAC ACC	CAC ACT TGG CGG TTC CTT CG
Ccl6	CCG GGC ATC ATC TTT ATC AGC A	TGA CAA TGC CTG CCC TCC TT
Ccl9	CAG CTG GGT CTG CCC ACT AA	CTC TGT TGC ATG TGT GAT CTG GG
Ccl11	TCC ATC TGT CTC CCT CCA CCA	AAG TTG GGA TGG AGC CTG GGT
Ccl17	ATG TAG GCC GAG AGT GCT GC	TGC ACA GAT GAG CTT GCC CT
Ccl20	AGG CAG AAG CAA GCA ACT ACG A	GCT TCA TCG GCC ATC TGT CTT G
Ccl22	CAA AAT CCT GCC GCA AGC CT	GCC TGG GAT CGG CAC AGA TA
Ccl24	CCA AGG CAG GGG TCA TCT TCA TC	TTG GCC CCT TTA GAA GGC TGG
Cxcl2	ACT GAA CAA AGG CAA GGC TAA CTG	AGA CAG CGA GGC ACA TCA GG
Cxcl9	TGC CAT GAA GTC CGC TGT TCT	AGG GTT CCT CGA ACT CCA CAC T
Cxcl10	CCA CGT GTT GAG ATC ATT GCC A	TGC GTG GCT TCA CTC CAG TT
Il17a	TGG ACT CTC CAC CGC AAT GA	TCC AGC TTT CCC TCC GCA TT
Ifng	GTT TGA GGT CAA CAA CCC ACA GG	GCG ACT CCT TTT CCG CTT CC
Tnfa	CAG GCG GTG CCT ATG TCT CA	GCC ATT TGG GAA CTT CTC ATC CC
Csf2	AAC TCC GGA AAC GGA CTG TGA	CTG GCC TGG GCT TCC TCA TT
Il1b	CCC CAA AAG ATG AAG GGC TGC	TGC CTG CCT GAA GCT CTT GT
Il6	ATT CTG CTC TGG AGC CCA CC	GCA ACT GGA TGG AAG TCT CTT GC
Il10	GCG CTG TCA TCG ATT TCT CCC	TGG CCT TGT AGA CAC CTT GGT C
Il12a	TGA CAT GGT GAA GAC GGC CA	ATG TGC TGG TTT GGT CCC GT
Il23a	TGT GCC CCG TAT CCA GTG TG	TCC TTT GCA AGC AGA ACT GGC
Ifnb1	TCA ACC TCA CCT ACA GGG CG	CAT TCC ACC CAG TGC TGG AGA
Tgfb1	ACT CCC GTG GCT TCT AGT GC	ACA GGA TCT GGC CAC GGA TG
Gapdh	TCG GTG TGA ACG GAT TTG GC	TGA AGG GGT CGT TGA TGG CAA